



OPEN Pyrotinib promotes the antitumor effect of T-DM1 by increasing drug endocytosis in HER2-positive breast cancer

Wenjun Ren^{1,5}, Tienian Zhu^{1,2,5}✉, Jiankun Liu²✉, Ruijing Zhao³, Fei Zhao¹, Yimei Zhang² & Jianping Mu⁴

Anti-HER2 therapy is integral to the treatment of HER2-positive breast cancer, but drug resistance hampers its effectiveness. Although antibody-drug conjugates (ADCs) are increasingly used in clinical practice, their application is often hindered by adverse reactions and drug resistance. Therefore, it is crucial to enhance the bioavailability of ADCs and reduce their dosages to mitigate both adverse effects and resistance. Pyrotinib's effect on HER2-positive breast cancer cell lines (SK-BR-3 and JIMT-1) was investigated via western blot, focusing on HER2 and downstream pathways. Pyrotinib's influence on HER2 ubiquitination and internalization was assessed through RT-qPCR, western blot, and immunofluorescence. The ability of pyrotinib to augment trastuzumab emtansine (T-DM1) endocytosis and antiproliferative effects was studied via CCK-8 and immunofluorescence. In vivo experiments in nude mice were conducted to explore the therapeutic efficacy of T-DM1 combined with pyrotinib. The single-drug study showed that pyrotinib downregulated HER2 protein levels and HER2 downstream signaling pathways. The mechanism of downregulating HER2 protein levels involved the promotion of HER2 internalization and degradation through the ubiquitin-proteasome pathway. The two-drug combination study showed that pyrotinib promoted the endocytosis of T-DM1, which improved its bioavailability. Increased cellular uptake further enhanced the antitumor effects of T-DM1 in both in vitro and in vivo experiments. Our results reveal the molecular mechanism by which pyrotinib regulates HER2 levels by promoting HER2 internalization, thereby facilitating the endocytosis of T-DM1. These findings suggest a potential combination treatment strategy for the targeted therapy of HER2-positive breast cancer.

Keywords Breast cancer, Human epidermal growth factor receptor 2, Tyrosine kinase inhibitor, Trastuzumab emtansine, Endocytoses

Abbreviations

ADC	Antibody-drug conjugates
T-DM1	DM1 trastuzumab emtansine
TKI	Tyrosine kinase inhibitors
qRT-PCR	Quantitative real-time polymerase chain reaction
UPS	Ubiquitin–proteasome pathway
ALP	Autophagy–lysosome pathway

Breast cancer is the most diagnosed type of cancer in women worldwide. According to the 2020 Global Cancer Epidemiological Survey, it has become the cancer type with the highest incidence and ranks as the fifth leading cause of cancer-related deaths globally¹. The incidence and mortality rates of breast cancer continue to rise, contributing to a significant global medical burden². Breast cancer is a molecularly heterogeneous disease,

¹Department of Oncology, Hebei Medical University, Shijiazhuang 050017, Hebei, China. ²Department of Medical Oncology, Bethune International Peace Hospital, Shijiazhuang 050082, Hebei, China. ³Department of Immunology, Key Laboratory of Immune Mechanism and Intervention on Serious Disease in Hebei Province, Hebei Medical University, Shijiazhuang 050017, Hebei, China. ⁴Department of Oncology, Shengji Cancer Hospital, Handan 056000, Hebei, China. ⁵Wenjun Ren and Tienian Zhu contributed equally to this work. ✉email: zhutienian2023@outlook.com; liujiankun1982@163.com

exhibiting distinct clinical characteristics and prognoses across different subtypes³. Among these subtypes, HER2-positive breast cancer—characterized by ERBB2 amplification and/or HER2 overexpression—is notable for its high invasiveness, high recurrence rate, and poor clinical prognosis⁴. It constitutes approximately 15–20% of all breast cancers⁵. HER2 is a member of the epidermal growth factor receptor family, which activates downstream PI3K and MAPK pathways through receptor homodimers and heterodimers, thereby playing key roles in regulating cell proliferation, differentiation, migration, and tumorigenesis⁶. Therefore, HER2 and its downstream pathways have become key targets in the treatment of breast cancer⁷.

The rapid progress in molecular biology and drug innovation has led to the development of HER2-targeting agents, marking a major milestone in drug discovery by effectively altering the natural course of HER2-positive breast cancer⁸. At present, three primary HER2-targeting strategies are used in clinical practice: monoclonal antibodies, tyrosine kinase inhibitors (TKIs), and antibody-drug conjugates (ADCs)⁷. Trastuzumab, a humanized monoclonal antibody that binds to the extracellular domain of HER2, remains the primary drug that successfully targets the HER2 pathway in clinical practice⁹. However, around 66–88% of HER2-positive metastatic breast cancer cases do not respond to initial trastuzumab treatment^{10,11}. Additionally, most patients who initially respond to trastuzumab develop secondary resistance within a year¹². Therefore, it is important to develop novel therapeutic strategies to overcome trastuzumab resistance.

Trastuzumab emtansine (T-DM1), the first ADC approved for HER2-positive breast cancer, consists of trastuzumab that is stably linked to the cytotoxic microtubule inhibitor DM1¹³. In vivo, the Fab region of the antibody component of the ADC recognizes and binds to the target cell-surface antigen¹⁴. Subsequently, the ADC-antigen complex undergoes internalization, releasing the cytotoxic drug to eliminate tumor cells¹⁵. The Phase III EMILIA study in HER2-positive advanced breast cancer showed that T-DM1 significantly improves progression-free survival (PFS) and overall survival (OS) compared to lapatinib plus capecitabine, with the most common grade 3/4 adverse events being thrombocytopenia (12.9%) and elevated liver enzymes (7.2%)¹⁶. Similarly, a study on T-DM1 for residual invasive HER2-positive breast cancer (NEJM 380, 2019) showed a 50% reduction in disease recurrence risk compared to trastuzumab, with grade 3/4 adverse events including thrombocytopenia (13%) and elevated liver enzymes (3%)¹⁷.

As the exploration of T-DM1 has expanded, its widespread use has been limited by the lack of superiority over control arms in various trials. Exploring novel strategies to improve the efficacy and safety of ADC drugs could offer enhanced clinical benefits for selected patients. Based on the mechanism of ADC drugs, increasing drug endocytosis presents a potential approach to amplify their potency. It has been shown that the irreversible TKI neratinib induces HER2 internalization and enhances the endocytosis of ADC, thereby bolstering the antitumor efficacy in lung cancer cell lines¹⁸. Pyrotinib, also an irreversible tyrosine kinase inhibitor, is a small-molecule tyrosine kinase inhibitor that irreversibly binds to the intracellular kinase domain of EGFR, HER2, and HER4 within the ATP pocket, thereby leading to the inhibition of tyrosine kinase activity¹⁹. Several clinical trials have demonstrated that pyrotinib, as a monotherapy or in combination with capecitabine, exhibits substantial therapeutic benefits in trastuzumab-resistant breast cancer cases^{20,21}. However, there have been no studies investigating whether pyrotinib possesses similar functions—inducing internalization of the HER2 protein and augmenting the efficacy of T-DM1 in HER2-positive breast cancer. This study aimed to elucidate the mechanisms underlying pyrotinib's effects on HER2-positive breast cancer cells and its potential for enhancing T-DM1 efficacy. The objective was to provide insights for future clinical trials and to establish a theoretical foundation for expanding the array of anti-HER2 therapeutic drugs and combination regimens available to medical professionals.

Materials and methods

Cell culture and reagents

We selected HER2-positive human breast cancer cell lines (SK-BR-3 and JIMT-1) which were kindly provided by the Beijing Institute of Genomics, Chinese Academy of Sciences. SK-BR-3 and JIMT-1 cells were cultured in RPMI 1640 medium (Gibco, Carlsbad, CA, USA) containing 10% fetal bovine serum (FBS; BI, Israel) and maintained in a humidified incubator (Thermo Fisher Scientific, USA) at 37 °C with 5% CO₂. Pyrotinib (Jiangsu HengRui Medicine Co. LTD, Lianyungang, Jiangsu, China) was dissolved in deionized water, while Lapatinib, MG-132, Velcade (Selleck Chemicals, Houston, TX, USA), and Bafilomycin A1 (MedChemExpress, Monmouth Junction, NJ, USA) were dissolved in dimethyl sulfoxide (DMSO). All reagents were stored at –80 °C.

Cell proliferation assays

Cell viability was assessed using the CCK-8 assay. SK-BR-3 and JIMT-1 cells were plated in 96-well plates (3–4 × 10³ cells/well) and exposed to different drug concentrations for 24 h. Afterward, 10 μL CCK-8 solution (Shanghai share-bio Biotechnology Co., Ltd.) was added to each well containing 100 μL of medium and incubated for 1–4 h at 37 °C. The absorbance was then measured at 450 nm using an enzyme-labeled instrument (Thermo Fisher Scientific, USA).

Cell scratching experiment

SK-BR-3 and JIMT-1 cells were seeded in 35 mm culture dishes, and after cell attachment, they were starved for 6 h. They were divided into the control group, T-DM1 group, T-DM1 combined with pyrotinib group, and T-DM1 combined with lapatinib group. Wounds were made along a ruler with a 10 μl pipette tip, and photographs were taken 24 h after drug treatment.

Western blot

SK-BR-3 and JIMT-1 cells were lysed in RIPA lysis buffer (Beijing Suolaibao Technology Co. Ltd, Beijing, China). Following protein quantification via the BCA method (Thermo Fisher Scientific, USA), 20–30 μg of protein was

separated on 10% SDS-PAGE gels and then transferred to PVDF membranes (Millipore, USA). After blocking with 5% nonfat milk or 3% bovine serum albumin (BSA), the membranes were incubated at 4 °C overnight with the primary antibodies HER2 Rabbit mAb, Phospho-HER2 (Tyr1221/1222) Rabbit mAb, Phospho-p44/42 MAPK (Erk1/2) (Thr202/Tyr204) Rabbit mAb, and Phospho-Akt (Ser473) Rabbit mAb, which were purchased from Cell Signaling Technology (Beverly, MA, USA). Akt Rabbit pAb and GAPDH Rabbit pAb were obtained from Wuhan Sanying Biotechnology (Wuhan, China), and Erk1/2 Rabbit pAb was obtained from Santa Cruz Biotechnology (Santa Cruz, CA). HER3 Rabbit mAb and Phospho-HER3 (Y1289) Rabbit mAb were obtained from Abways Technology (Shanghai, China). Subsequently, the membranes were incubated with a secondary antibody (Goat Anti-Rabbit IgG (H + L) HRP) (Shanghai Abways Biotechnology Co., Ltd., Shanghai, China) for 1.5 h at room temperature. Finally, the membranes were developed using Beyo ECL Plus (Beyotime Institute of Biotechnology, Shanghai, China) and exposed on X-ray film (Kodak, USA).

Quantitative real-time polymerase chain reaction (qRT-PCR)

Total RNA was extracted using Trizol (Life Technologies, USA) and subsequently reverse-transcribed into cDNA using the PrimeScript™ RT reagent Kit with gDNA Eraser (Takara, Dalian, China). Real-time PCR was conducted using TB Green™ Premix Ex Taq™ II (Tli RNaseH Plus) (Takara, Dalian, China) on a Cobas Z480 automatic fluorescence quantitative PCR analyzer (Roche Diagnostics, Basel, Switzerland). The primer sequences for qRT-PCR were as follows: HER2: HER2-F: TGTGACTGCCTGTCCCTACAA; HER2-R: CCAGACCATAGCACACTCGG; GAPDH: GAPDH-F: GGAGCGAGATCCCTCCAAAAT; GAPDH-R: GGCTGTTGTCAT-ACTTCTCATGG. The relative mRNA expression of HER2 was quantified using the $\Delta\Delta C_t$ method, with GAPDH serving as the internal control.

Coimmunoprecipitation

Cell lysates were prepared using IP lysis buffer (Beyotime Institute of Biotechnology, Shanghai, China) containing protease inhibitors. They were then incubated with HER2 mouse mAb (Santa Cruz Biotechnology, Santa Cruz, CA) and normal mouse IgG (Santa Cruz Biotechnology, Santa Cruz, CA) on a shaker at 4 °C overnight. Following this conjugation step, Protein A/G PLUS-Agarose (Santa Cruz Biotechnology, Santa Cruz, CA) was added and allowed to incubate for an additional 8 h at 4 °C. Protein-antibody complexes were collected after centrifugation and subjected to washing steps with IP lysis buffer (50 mM Hepes, 0.1% Triton X-100), 0.5 M NaCl in Hepes/Triton X-100, and IP wash buffer. The immunoprecipitated proteins were subsequently separated by 8% SDS-PAGE and analyzed by western blot.

Immunofluorescence

To observe HER2 internalization, cells were cultured on cover slips in 24-well cell culture plates. After being treated with pyrotinib and lapatinib, the cells were fixed with 4% paraformaldehyde, permeabilized with 0.1% Triton X-100, and incubated with a blocking solution and HER2 Rabbit mAb (Cell Signaling Technology) at 4 °C overnight. Subsequently, the cells were incubated with Goat Anti-Rabbit IgG (H + L) Alexa Fluor 488 (Shanghai Abways Biotechnology Co., Ltd., Shanghai, China) for 1 h at room temperature. The coverslips were then sealed onto slides using an anti-fluorescence quenching agent with DAPI at 4 °C, protected from light, and observed using confocal microscopy (Nikon A1R, Nikon Instruments Inc.).

To confirm that pyrotinib promotes an increase in T-DM1 endocytosis, the following steps were undertaken. After mounting the slices, the cells were exposed to T-DM1, which had been labeled using the pHrodo™ Deep Red Antibody labeling kit (Thermo Fisher Scientific, USA), following the manufacturer's instructions. Following a 30-minute incubation period, pyrotinib was added. Finally, the cells were fixed with 4% paraformaldehyde and sealed using an anti-fluorescence quenching agent with DAPI. Images were then acquired using confocal microscopy.

Xenograft mouse model

JIMT-1 cells (6×10^6) were subcutaneously injected into 6-week-old female BALB/c nude mice (Beijing Vital River Laboratory Animal Technology Co., Ltd., Beijing, China) to establish xenograft tumors. Once the tumor volume reached 50–100 mm³ (calculated as tumor volume = $1/2$ (long diameter \times short diameter²)), the mice were randomly assigned to four treatment groups ($n = 6$ per group). The control group received sterilized water 5 days a week; the pyrotinib group was administered pyrotinib (2 mg/kg) via oral gavage 5 days a week; the T-DM1 group received T-DM1 (10 mg/kg) through tail vein injection once every 3 weeks; and the combination therapy group was treated with pyrotinib and T-DM1 at the same dosage and administration schedule as previously mentioned. The mouse body weight and tumor volume were measured every 3 days. After 3 weeks of treatment, the nude mice were euthanized by cervical dislocation, and their tumor tissues were dissected, weighed, and either formalin-fixed for immunohistochemistry (IHC) or snap-frozen in liquid nitrogen for western blot analysis. Methods involving animal work were approved by the Ethics Committee of Bethune International Peace Hospital (protocol code DWsy-22-12-10). All methods were performed in accordance with the ARRIVE guidelines. All experiments were performed in accordance with relevant guidelines and regulations.

Immunohistochemistry

The fixed tumor tissues were embedded in paraffin, and 4- μ m-thick sections were prepared. The sections were then stained with hematoxylin-eosin (HE) and subjected to IHC staining for HER2. Anti-HER2/neu (4B5) Rabbit Monoclonal Primary Antibody (Roche Diagnostics, Basel, Switzerland) was employed to detect the protein levels in the xenograft tissues.

Statistical analysis

GraphPad Prism 8 software was used for graph creation, and all data were analyzed using SPSS 19 statistical software (SPSS, Inc. Chicago, IL). The quantitative data were presented as mean \pm standard deviation. For multiple-group comparisons, one-way analysis of variance (ANOVA) with Dunnett's post-hoc test was performed. The significance level was set at $\alpha = 0.05$, with a P value lower than 0.05 considered statistically significant.

Results

Pyrotinib downregulates HER2 protein levels and inhibits the phosphorylation of the PI3K/AKT and RAS/MAPK signaling pathways in HER2-positive breast cancer cells

We treated HER2-positive breast cancer cells with the irreversible HER2-TKI pyrotinib and the reversible HER2-TKI lapatinib to observe their respective impacts on HER2 protein levels and downstream signaling pathways. SK-BR-3 and JIMT-1 cells were exposed to different concentrations and durations of pyrotinib and lapatinib treatment. The results showed a gradual decrease in HER2 protein levels with increasing concentrations of pyrotinib and prolonged intervention time, accompanied by decreased levels of p-HER2, p-AKT, and p-ERK in the cells. (Fig. 1c and d) Conversely, as the concentration of lapatinib increased and the intervention time was prolonged, the expression level of HER2 protein showed an upward trend, consistent with previous reports, while the expression levels of p-HER2, p-AKT, and p-ERK decreased gradually^{18,22}. (Fig. 1a and b) When comparing the phosphorylation levels of HER2 downstream pathways after treatment with both drugs, JIMT-1 cells showed a less pronounced decrease in PI3K/AKT pathway phosphorylation than SK-BR-3 cells. This phenomenon may be related to the presence of a rare mutation in PIK3CA in JIMT-1 cells, which has been shown to strongly activate downstream signaling pathways^{23,24}.

We further assessed HER3 and p-HER3 levels under the same treatment conditions, given their role in HER2-mediated PI3K/AKT signaling. The results showed differential regulation by pyrotinib and lapatinib in both cell lines (Supplementary Figure S1).

The mechanism by which pyrotinib induces HER2 degradation in HER2-positive breast cancer cells

To further investigate the underlying mechanism behind the changes in HER2 protein levels, we employed qRT-PCR to assess the impact of pyrotinib and lapatinib on HER2 mRNA expression. The results showed that after treatment with pyrotinib and lapatinib at various time points, the expression levels of HER2 mRNA in SK-BR-3 and JIMT-1 cells progressively increased (Fig. 2a). The findings imply that lapatinib may elevate HER2 protein levels through transcriptional upregulation, whereas the mechanism underlying the decrease in HER2 levels induced by pyrotinib may operate post-transcriptionally and could involve protein degradation.

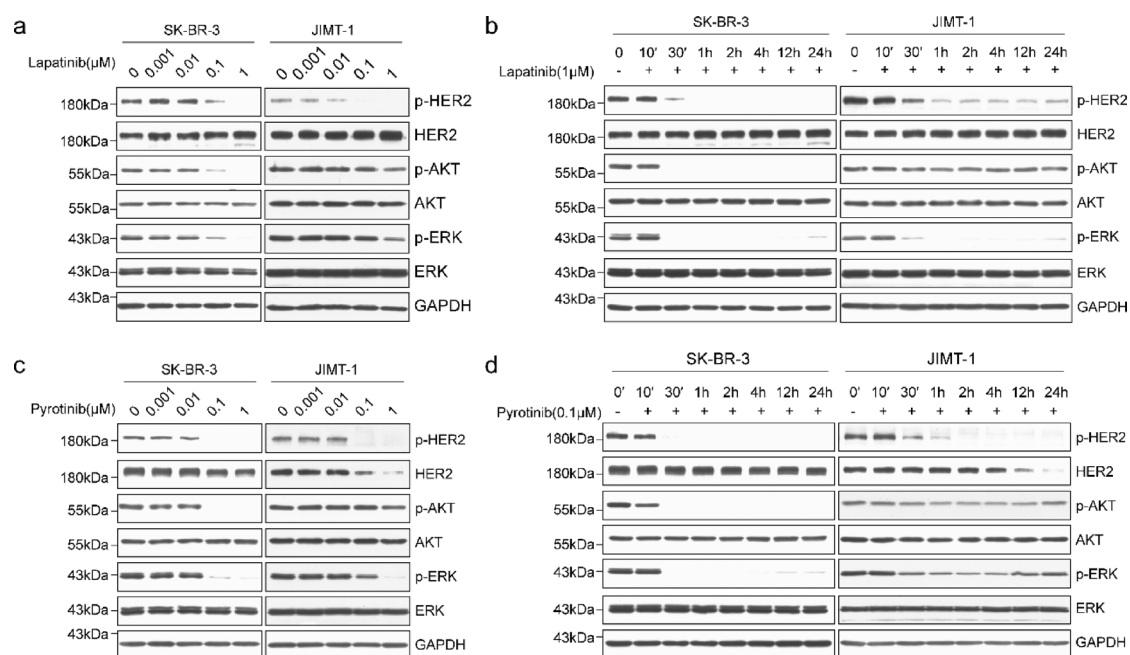


Fig. 1. Pyrotinib downregulates HER2 protein levels and suppresses phosphorylation of HER2, PI3K/AKT, and RAS/MAPK signaling pathways in SK-BR-3 and JIMT-1 cells. (a–d) Expression levels of HER2 and its downstream proteins in the PI3K/AKT and RAS/MAPK signaling pathways were analyzed by western blotting. (a) Both cell types were treated with lapatinib (0.001, 0.01, 0.1, 1 μ M) for 24 h. (b) Both cell types were treated with lapatinib (1 μ M) at different time points. (c) Both cell types were treated with pyrotinib (0.001, 0.01, 0.1, 1 μ M) for 24 h. (d) Both cell types were treated with pyrotinib (0.1 μ M) at different time points. Results are representative of 3 independent replicates.

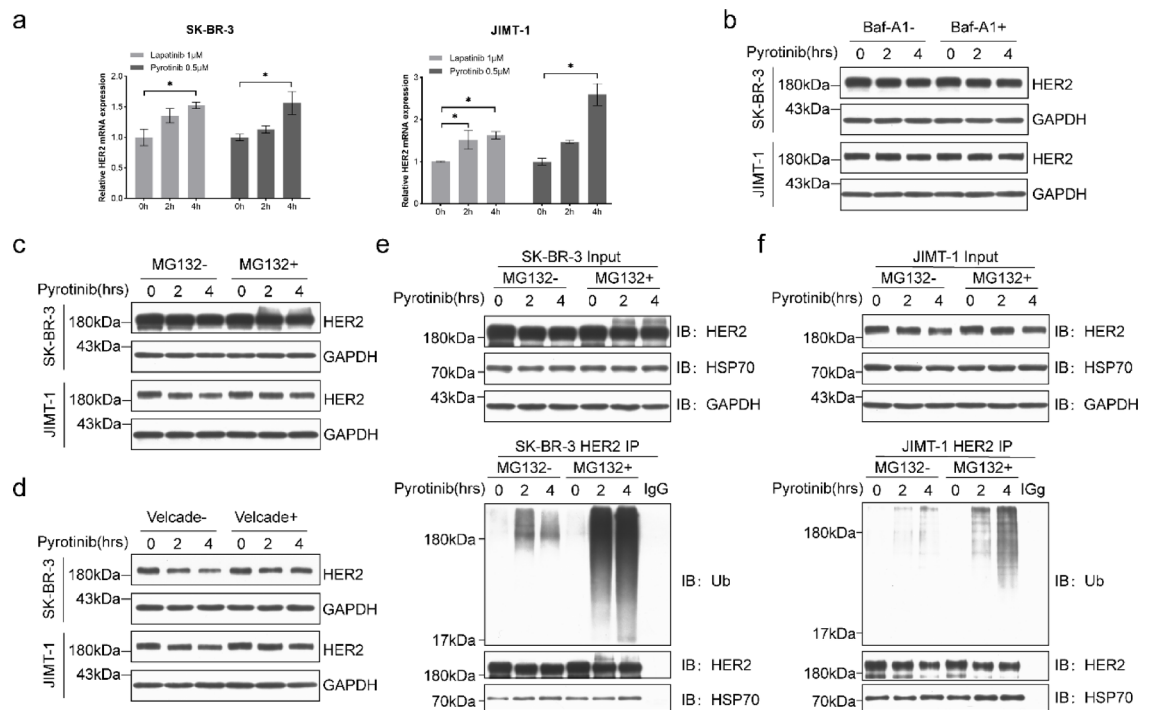


Fig. 2. Pyrotinib promotes HER2 degradation via the ubiquitin–proteasome pathway. **(a)** HER2 mRNA expression in SK-BR-3 and JIMT-1 cells treated with pyrotinib (0.5 μM) or lapatinib (1 μM) as assessed using RT-qPCR. **(b–d)** SK-BR-3 and JIMT-1 cells were treated with the lysosomal inhibitor Baf-A1 (20 nM) or proteasome inhibitors Velcade (0.5 μM) or MG-132 (10 μM) for 0.5 h, with DMSO as the control, followed by the addition of pyrotinib (0.5 μM) for 0, 2, and 4 h. **(e–f)** Cells were subjected to MG132 (10 μM) treatment for 0.5 h or DMSO as the control, followed by the addition of pyrotinib (0.5 μM) for 0, 2, and 4 h. HER2 was immunoprecipitated from the lysates, and the samples were analyzed by immunoblotting with an anti-ubiquitin, anti-HER2, and anti-HSP70 antibodies. GAPDH served as the loading control. Results are representative of 3 independent replicates.

Protein degradation primarily occurs through two pathways: the ubiquitin–proteasome pathway (UPS) and the autophagy–lysosome pathway (ALP)^{25,26}. To ascertain whether pyrotinib-induced downregulation of HER2 protein levels occurs via modulation of HER2 degradation, we pretreated the two cell lines with proteasome inhibitors (MG132 or Velcade) and lysosome inhibitors (Baf-A1) for 30 min. Subsequently, pyrotinib was administered at different time points (0, 2, and 4 h). We observed that the degradation of HER2 protein was inhibited following the administration of Velcade or MG132 (Fig. 2c and d), while the addition of Baf-A1 had no effect on the declining trend in HER2 protein levels (Fig. 2b). This indicates that the reduction in HER2 protein levels induced by pyrotinib results from enhanced degradation via the ubiquitin–proteasome system.

The molecular chaperone system plays a crucial role in maintaining protein homeostasis. HSP70 belongs to the molecular chaperone family. Previous studies have shown that substrate proteins that cannot be repaired bind to HSP70 and enter the ubiquitin–proteasome system for degradation²⁷. This prompted us to hypothesize whether pyrotinib induces HER2 ubiquitination through enhanced association of HER2 with HSP70. Consequently, coimmunoprecipitation experiments were conducted, revealing that the addition of pyrotinib resulted in elevated HER2 ubiquitination levels and enhanced binding between HSP70 protein and HER2 (Fig. 2e and f).

Pyrotinib facilitates the internalization of HER2 and the endocytosis of T-DM1

In the immunofluorescence experiment, we assessed the effects of pyrotinib and lapatinib on HER2 using laser confocal microscopy. The results indicated that, in the absence of drug treatment, immunofluorescent staining of HER2 predominantly localized on the cell membrane. Upon treatment with pyrotinib, the distribution of HER2 on the cytoplasmic membrane notably decreased, with aggregates appearing submembranously and within the cytoplasm. Conversely, lapatinib induced an increase in HER2 accumulation on the cell surface. This result is consistent with previous studies showing that lapatinib can increase the surface expression of HER2 in cells^{18,22}. These findings suggest that the irreversible HER2-TKI pyrotinib may induce internalization of HER2 (Fig. 3a). This result is consistent with previous studies demonstrating that neratinib induces the internalization of HER2 on the cell surface^{18,28}.

Furthermore, we explored whether pyrotinib could enhance the endocytosis of T-DM1, which binds to HER2. Fluorescence staining was employed to label T-DM1, and its endocytosis was observed. Upon the addition of pyrotinib, the level of T-DM1 endocytosis into cells increased compared to the absence of pyrotinib, demonstrating that pyrotinib can augment the cellular uptake of T-DM1 (Fig. 3b).

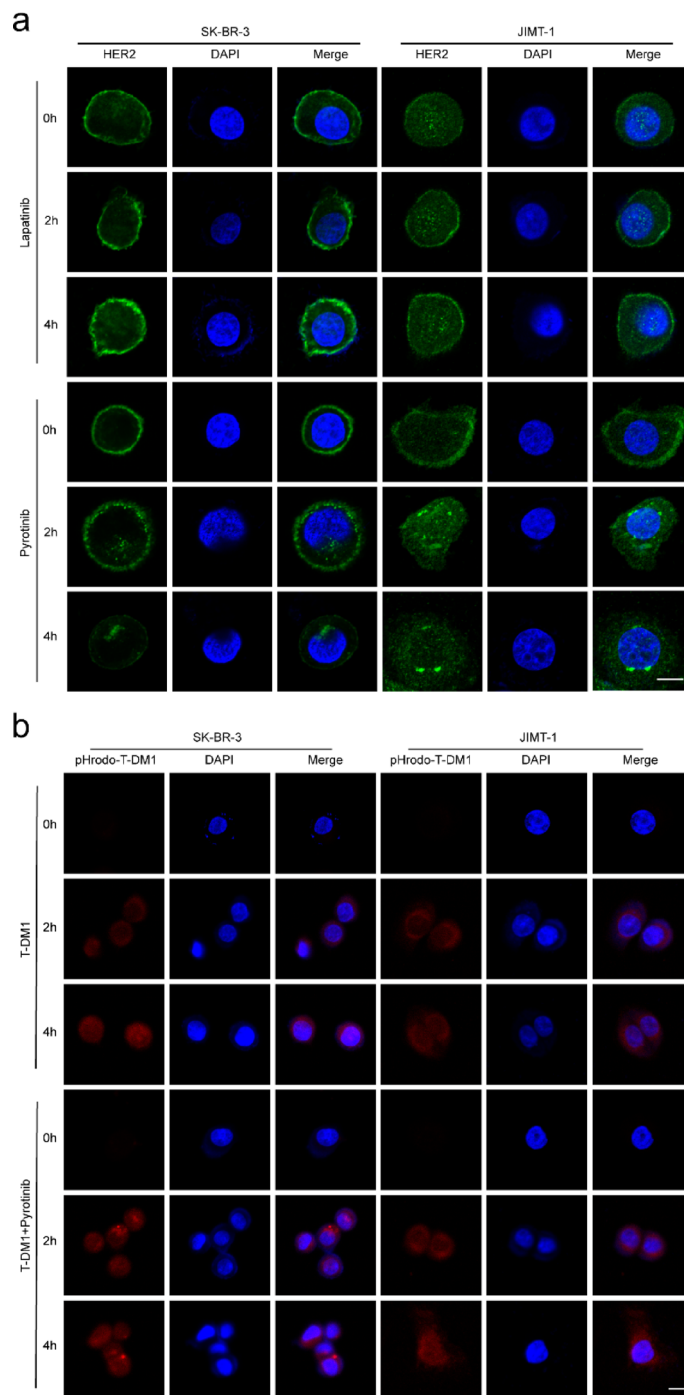


Fig. 3. Pyrotinib promotes HER2 internalization and T-DM1 endocytosis. **(a)** Cells were treated with pyrotinib (0.5 μ M) or lapatinib (1 μ M) for 0, 2, and 4 h and processed for immunofluorescence experiments using anti-HER2 antibody (green). Nuclei were stained with DAPI (blue) ($\times 1000$), Scale bar = 10 μ m. **(b)** After labeling T-DM1 with pHrodo Deep Red (pHrodo-T-DM1), the cells were exposed to pHrodo-T-DM1 (1 μ g/mL) alone or in combination with pyrotinib (0.1 μ M) for 0, 2, and 4 h. pHrodo-T-DM1 emits red fluorescent signals within the cellular interior. Nuclei were stained with DAPI (blue) ($\times 600$). The quantification of T-DM1 fluorescence intensity is now shown in Supplementary Figure S2. Scale bar = 10 μ m. Results are representative of 3 independent replicates.

Pyrotinib augments the anti-proliferative effect of T-DM1 in HER2-positive breast cancer cells

To investigate whether increased endocytosis of T-DM1 induced by pyrotinib enhances its inhibition of cell proliferation, CCK8 experiments were conducted to compare the inhibitory effects on proliferation of T-DM1 alone versus T-DM1 in combination with pyrotinib or lapatinib. Initially, standalone CCK8 experiments with

pyrotinib or lapatinib were performed to determine the minimum effective concentration. Subsequently, experiments were conducted using the selected drug concentrations of pyrotinib and lapatinib, either in combination with or without T-DM1. The results revealed that the combination of pyrotinib and T-DM1 showed superior growth inhibition compared to T-DM1 alone. However, there was no significant difference in the cell growth inhibition rate between T-DM1 combined with lapatinib and T-DM1 alone. These experimental findings demonstrate that pyrotinib, at doses lacking cytostatic effects, can synergistically enhance the cytotoxicity of T-DM1 (Fig. 4a and b). To further assess the broader applicability of these findings, we also conducted cell proliferation assays in BT474 and MDA-MB-453 cells. The results were consistent with those observed in SK-BR-3 and JIMT-1 cells, and are provided in Supplementary Figure S3. Furthermore, the cell scratch experiment treated two cell lines with a fixed concentration of T-DM1 combined with either lapatinib or pyrotinib to assess their impact on migration ability. Following 24 h of drug exposure, migration rates were quantified. Results demonstrated that the combination of T-DM1 and pyrotinib significantly suppressed migration rates of SK-BR-3 and JIMT-1 cells compared to the control group, whereas the T-DM1 and lapatinib combination did not exhibit significant inhibition of cell migration. This suggests that coadministration with pyrotinib enhances T-DM1's efficacy in impeding the migration of SK-BR-3 and JIMT-1 cells (Fig. 4c).

Subsequently, *in vivo* experiments were conducted to evaluate the antitumor efficacy of the combination therapy using the JIMT-1 xenograft tumor model. The monotherapy group exhibited limited inhibition of tumor volume growth compared to the control group, whereas the combined treatment group demonstrated significantly stronger inhibitory effects compared to the monotherapy group (Fig. 5a-c). There were no significant differences in the body weight of the nude mice among the groups throughout the study period (Fig. 5d). These findings suggest that the combination therapy involving T-DM1 and pyrotinib demonstrates enhanced efficacy *in vivo* without additional toxic side effects.

Immunohistochemical (IHC) analysis was performed to assess HER2 protein expression in dissected tumor tissues. HER2 staining in tumor tissues from the monotherapy group showed a reduction compared to the control group, whereas a significant reduction was observed in the combination treatment group (Fig. 5e). Western blot analysis of HER2 protein levels in the four groups of tumor tissues showed trends consistent with the IHC findings. These findings suggest that both T-DM1 and pyrotinib can decrease HER2 protein levels, with their combination further enhancing HER2 protein degradation. Consistent *in vitro* results showed T-DM1 reduced HER2 levels in a dose-dependent manner (Supplementary Figure S4). Additionally, the phosphorylation levels of downstream signaling pathways, including P-HER2, P-AKT, and P-ERK, were notably lower in the combination treatment group compared to the other groups (Fig. 5f).

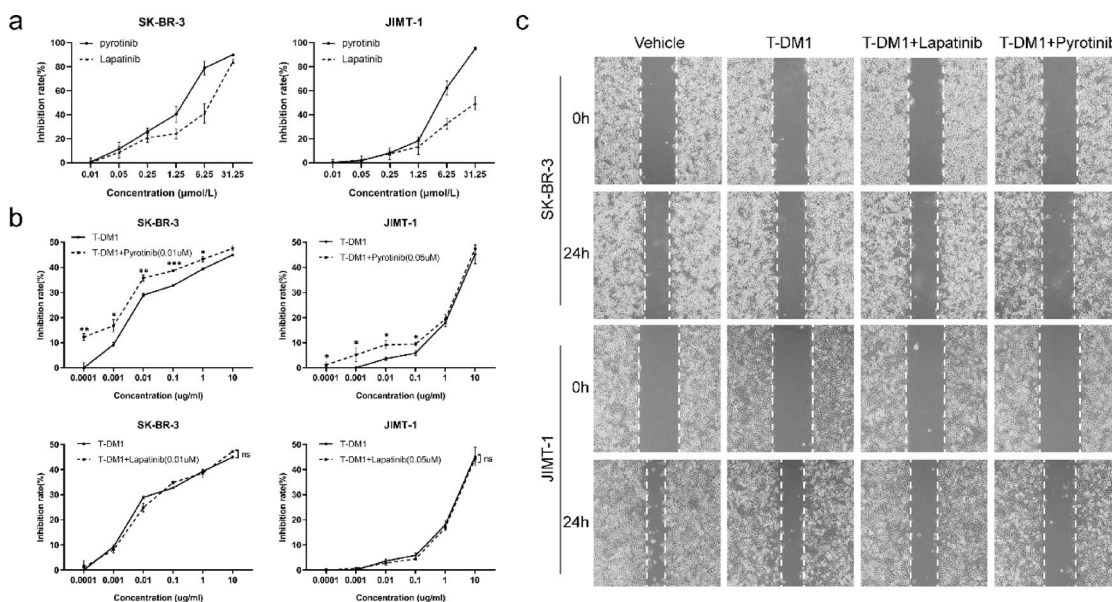


Fig. 4. Pyrotinib enhances the antitumor effect of T-DM1 *in vitro*. **(a)** The effects of various concentrations of pyrotinib and lapatinib on the viability of SK-BR-3 and JIMT-1 cells. Cell viability was assessed using a CCK-8 assay after 24 h. Y-axis: The Inhibition Ratio (%) represents the percentage of cell proliferation inhibition compared to untreated/control cells. **(b)** Cells were treated with T-DM1 (0.0001, 0.001, 0.01, 0.1, 1, 10 μg/mL) either alone or in combination with pyrotinib or lapatinib (SK-BR-3:0.01 μM, JIMT-1:0.05 μM). Cell viability was measured after 24 h of treatment. **(c)** Scratch assay to detect the effect of pyrotinib or lapatinib (SK-BR-3:0.01 μM, JIMT-1:0.05 μM) combined with T-DM1 (0.1 μg/mL) on the migration ability of breast cancer cells. Photograph the scratched area after 24 h. * $P < 0.05$, ** $P < 0.01$, *** $P < 0.001$, **** $P < 0.0001$, ns = not significant. Results are representative of 3 independent replicates.

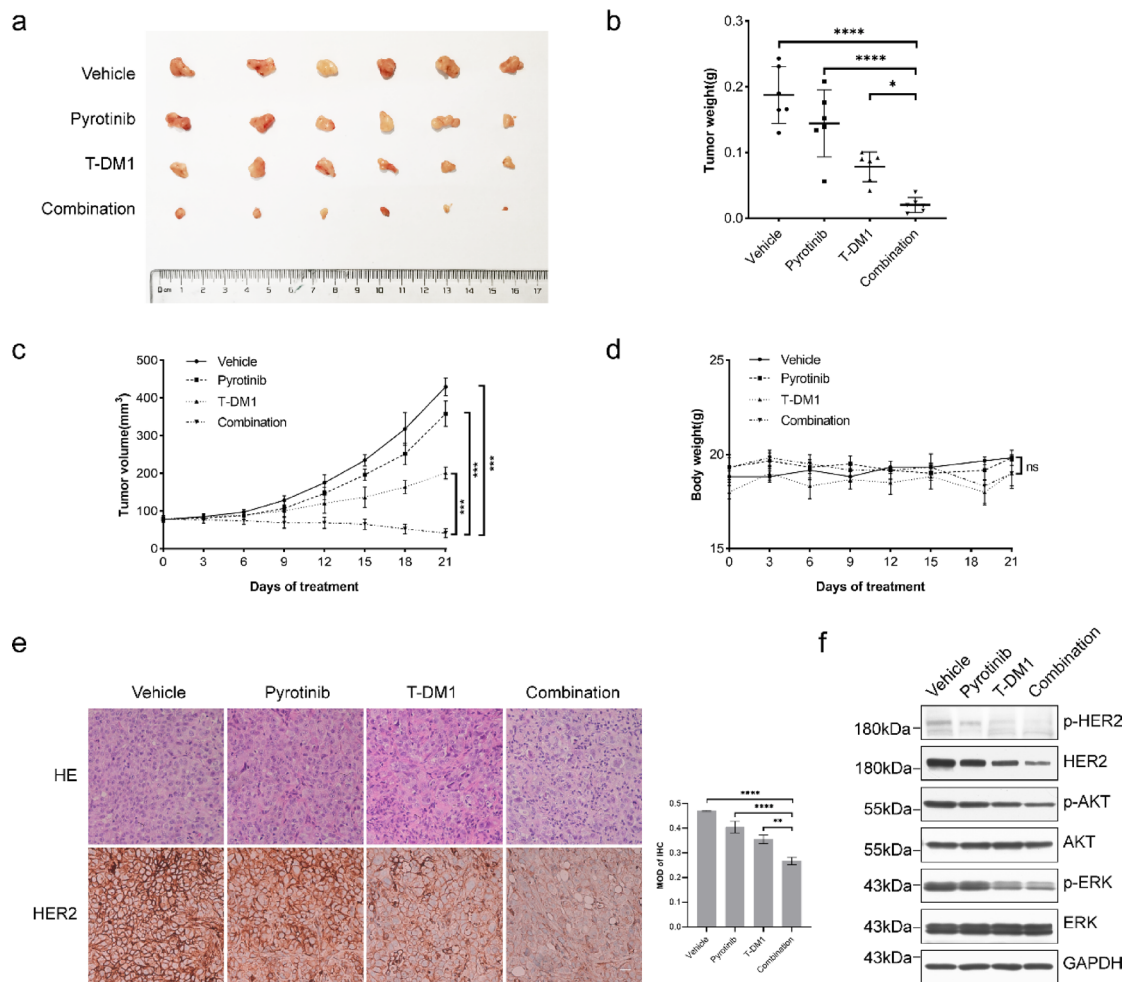


Fig. 5. Pyrotinib enhances the antitumor effect of T-DM1 in vivo. **(a)** Images of JIMT-1 xenografts harvested after 21 days of treatment with T-DM1 (10 mg/kg) with or without pyrotinib (2 mg/kg) ($n=6$). **(b)** Changes in tumor weight in the examined mice. **(c)** Changes in tumor volume in the examined mice. **(d)** Body weight changes in mice after treatments. **(e)** Representative images displaying HE and IHC staining of xenograft tumor tissues ($\times 400$), scale bars = 50 μm . The histogram shows the average absorbance of HER2. **(f)** The protein expression levels of HER2 and its downstream signaling pathways in tumor tissues of each group were analyzed by western blot. GAPDH served as the loading control. * $P < 0.05$, ** $P < 0.01$, *** $P < 0.001$, **** $P < 0.0001$, ns = not significant. Results are representative of 3 independent replicates.

Discussion

The two cell lines used in this experiment, namely SK-BR-3 and JIMT-1, are both characterized as HER2-positive cell lines. Notably, JIMT-1 is a trastuzumab-resistant cell line²⁹. The results of the present study clearly show that pyrotinib can inhibit the phosphorylation levels of the MAPK and PI3K signaling pathways downstream of HER2 and reduce the expression levels of HER2 protein. Furthermore, this effect becomes more pronounced with increasing concentration and prolonged exposure—a phenomenon not documented in previous studies. Lapatinib is a reversible TKI, and its mechanism of action is different from that of pyrotinib. When using lapatinib as a control, the results showed that lapatinib promoted the increase in HER2 expression levels. These findings suggest that the effects on HER2 levels and downstream signaling are independent. A study conducted by Li et al. investigating HER2-positive lung cancer showed that irreversible TKIs, such as neratinib and afatinib, contributed to a decrease in HER2 protein levels, whereas reversible inhibitors such as lapatinib and tucatinib did not induce such an effect¹⁸. This is consistent with the results of the present study. In our in vivo experiments, we observed that T-DM1 decreases HER2 levels, consistent with its mechanism of action. T-DM1 binds to HER2, is internalized, and undergoes degradation, releasing its cytotoxic component. This reduction in HER2 levels likely results from this internalization and subsequent degradation.

Exploring the mechanism underlying the pyrotinib-induced alterations in HER2 levels within cells, we discovered that HER2 mRNA expression increased after drug treatment, confirming that pyrotinib did not hamper HER2 protein synthesis. Subsequent experiments involving proteasome inhibitors, lysosomal inhibitors, immunoprecipitation, and immunofluorescence showed that the amount of HSP70 bound to HER2 protein increased significantly with the prolongation of drug exposure time after the addition of pyrotinib. This occurrence

was concomitant with an elevation in ubiquitination levels, culminating in the translocation of HER2 from the cell membrane to the cytoplasm, followed by degradation through the UPS. Notably, the UPS predominantly identifies short-lived, misfolded, and impaired proteins, wielding a pivotal role in governing cell signaling, transcription, and processes such as cell cycle progression, survival, proliferation, and apoptosis³⁰. HSP70 belongs to the molecular chaperone family and plays a central role in diverse facets of protein homeostasis, from protein folding and assembly to degradation, acting as a caretaker²⁷. Previous studies have shown that substrate proteins that cannot be repaired in the UPS dissociate from HSP90, which maintains protein homeostasis, and bind to HSP70. Under the catalytic action of CHIP, an E3 ubiquitin ligase, the substrate is ubiquitinated and forms a ubiquitinated complex, which is then escorted to the proteasome by BAG-1, releasing the substrate protein. Finally, the substrate enters the proteasome for degradation²⁷. Xu et al. found that the ubiquitination degradation of HER2 depends on the binding of HER2 protein to HSP70 after dissociation from HSP90³¹. Moreover, Citri et al. found that the irreversible TKI CI-1033 could cause cysteine alkylation of HER2 receptors, accelerating their intracellular degradation by promoting the dissociation of HER2 from HSP90 and binding to HSP70, as well as accelerating internalization and ubiquitination degradation of HER2³².

ADCs, composed primarily of humanized monoclonal antibodies of the IgG class and chemically conjugated with a cytotoxic payload through a molecular linker, constitute an innovative therapeutic approach. Within the body, ADCs engage target antigens on cell surfaces via the antibody Fab region, prompting the entire ADC complex to undergo endocytosis into lysosomes. Within these lysosomes, the cytotoxic payload is released, triggering tumor cell demise. Simultaneously, the intact/wildtype Fc region mediates antibody-dependent cell-mediated cytotoxicity (ADCC), bolstering antitumor activity¹⁸. T-DM1—the inaugural ADC approved for breast cancer—is composed of the antigen-specific antibody trastuzumab and the cytotoxic chemotherapy agent DM1. This linkage is facilitated by a noncleavable linker, yielding a drug–antibody ratio of 3.5. While T-DM1 constitutes a standard treatment after trastuzumab resistance, the noteworthy incidence of hematological and hepatic toxicities still restricts its clinical implementation in certain patients. The antitumor activity of ADCs hinges on factors such as tissue distribution within tumors, cell-surface antigen expression, and endocytosis efficiency. Concurrently, ADCs' toxicity is linked with conjugate stability in the bloodstream and off-target effects of the payload^{15,33}. Developing strategies to augment T-DM1 efficacy, minimize daily drug dosages, and mitigate adverse reactions would amplify benefits for patients. T-DM1 exerts its cytotoxic effect by binding to the HER2 receptor and undergoing endocytosis into the cell³⁴. Previous studies have highlighted that HER2 ubiquitination and internalization are important mechanisms mediating ADC endocytosis, which contribute to the therapeutic effects of T-DM1¹⁸. Our work has demonstrated that pyrotinib is capable of inducing HER2 receptor internalization on the surface of breast cancer cells, thereby intensifying T-DM1's endocytic efficiency. In the CCK8 study and scratch assay, we observed that the use of non-cytotoxic doses of pyrotinib synergistically enhanced the cytostatic potency of T-DM1. The scratch assay results showed a significant reduction in tumor cell migration, suggesting that this combination may not only inhibit cell proliferation but also reduce metastasis. The absence of synergistic effects between lapatinib and T-DM1 could be due to lapatinib's augmentation of HER2 stability and accumulation on the plasma membrane^{18,35}.

For in vivo experiments, we selected the JIMT-1 cell line to establish a xenograft model. The experimental outcomes revealed that the combination of pyrotinib and T-DM1 outperformed monotherapy in terms of antitumor efficacy. IHC and western blot analyses of the tumor tissue corroborated that T-DM1 reduced HER2 expression, and this effect was further accentuated with the addition of pyrotinib. Notably, there were no significant differences in P-HER2, P-AKT, and P-ERK between the T-DM1 group and the combination group. This finding suggests that pyrotinib's synergistic effect on T-DM1 arises from its promotion of HER2 internalization and augmentation of T-DM1 endocytosis. Li et al. highlighted that neratinib augmented T-DM1's antitumor efficacy in HER2-positive lung cancer cells through the facilitation of HER2 internalization¹⁸. Additionally, case reports have shown the combination of pyrotinib and T-DM1 in HER2-negative metastatic breast cancer with HER2 mutations³⁶. Importantly, both neratinib and pyrotinib are classified as irreversible TKIs, further supporting the congruence with the results of our study. However, more recent studies, including those by Kulukian et al., have demonstrated that the reversible HER2 TKI tucatinib also enhances T-DM1 internalization and degradation³⁷, suggesting that the relationship between HER2 inhibitors and T-DM1 may be more complex than a simple reversible versus irreversible distinction. Furthermore, studies on other targeted therapies, such as the combination of trastuzumab and cilengitide, which inhibits integrins to disrupt cell adhesion and migration, have also demonstrated promising results in HER2-positive cancers, further supporting the potential of combining HER2-targeted therapies to improve treatment outcomes³⁸.

Conclusions

Pyrotinib can enhance HER2 internalization, thereby promoting increased T-DM1 endocytosis that is linked to HER2, and consequently enhancing the antitumor activity of T-DM1. The combination of these two drugs offers a theoretical basis for reducing the dosage of T-DM1 and mitigating its adverse reactions, while maintaining its efficacy. The combined therapy approach holds the potential to provide an effective treatment option for future clinical trials, ultimately leading to improved treatment outcomes for a broader patient population.

Data availability

The raw data supporting the conclusions of this article will be made available by the authors upon reasonable request.

Received: 8 October 2024; Accepted: 21 May 2025

Published online: 28 May 2025

References

- Sung, H. et al. Global cancer statistics 2020: GLOBOCAN estimates of incidence and mortality worldwide for 36 cancers in 185 countries. *CA Cancer J. Clin.* **71**, 209–249. <https://doi.org/10.3322/caac.21660> (2021).
- Arnold, M. et al. Current and future burden of breast cancer: global statistics for 2020 and 2040. *Breast* **66**, 15–23. <https://doi.org/10.1016/j.breast.2022.08.010> (2022).
- Johnson, K. S., Conant, E. F. & Soo, M. S. Molecular subtypes of breast cancer: A review for breast radiologists. *J. Breast Imaging* **3**, 12–24. <https://doi.org/10.1093/jbi/wbaa110> (2021).
- Najjar, M. K., Manore, S. G., Regua, A. T. & Lo, H. W. Antibody-Drug conjugates for the treatment of HER2-Positive breast Cancer. *Genes (Basel)* **13**. <https://doi.org/10.3390/genes13112065> (2022).
- Loibl, S. & Gianni, L. HER2-positive breast cancer. *Lancet* **389**, 2415–2429. [https://doi.org/10.1016/S0140-6736\(16\)32417-5](https://doi.org/10.1016/S0140-6736(16)32417-5) (2017).
- Tebbutt, N., Pedersen, M. W. & Johns, T. G. Targeting the ERBB family in cancer: Couples therapy. *Nat. Rev. Cancer* **13**, 663–673. <https://doi.org/10.1038/nrc3559> (2013).
- Swain, S. M., Shastry, M. & Hamilton, E. Targeting HER2-positive breast cancer: Advances and future directions. *Nat. Rev. Drug Discov.* **22**, 101–126. <https://doi.org/10.1038/s41573-022-00579-0> (2023).
- Tarantino, P., Morganti, S. & Curigliano, G. Targeting HER2 in breast cancer: New drugs and paradigms on the horizon. *Explor. Target. Antitumor Ther.* **2**, 139–155. <https://doi.org/10.37349/etat.2021.00037> (2021).
- Maadi, H., Soheilifar, M. H., Choi, W. S., Moshtaghian, A. & Wang, Z. Trastuzumab mechanism of action; 20 years of research to unravel a dilemma. *Cancers (Basel)* **13**. <https://doi.org/10.3390/cancers13143540> (2021).
- Vogel, C. L. et al. Efficacy and safety of trastuzumab as a single agent in first-line treatment of HER2-overexpressing metastatic breast cancer. *J. Clin. Oncol.* **20**, 719–726. <https://doi.org/10.1200/JCO.2002.20.3.719> (2002).
- Baselga, J. et al. Phase II study of weekly intravenous recombinant humanized anti-p185HER2 monoclonal antibody in patients with HER2/neu-overexpressing metastatic breast cancer. *J. Clin. Oncol.* **14**, 737–744. <https://doi.org/10.1200/JCO.1996.14.3.737> (1996).
- Nahta, R., Yu, D., Hung, M. C., Hortobagyi, G. N. & Esteva, F. J. Mechanisms of disease: Understanding resistance to HER2-targeted therapy in human breast cancer. *Nat. Clin. Pract. Oncol.* **3**, 269–280. <https://doi.org/10.1038/ncponc0509> (2006).
- Peddi, P. F. & Hurvitz, S. A. Trastuzumab emtansine: The first targeted chemotherapy for treatment of breast cancer. *Future Oncol.* **9**, 319–326. <https://doi.org/10.2217/fon.13.7> (2013).
- Tsuchikama, K. & An, Z. Antibody-drug conjugates: Recent advances in conjugation and linker chemistries. *Protein Cell* **9**, 33–46. <https://doi.org/10.1007/s13238-016-0323-0> (2018).
- Drago, J. Z., Modi, S. & Chandarlapaty, S. Unlocking the potential of antibody-drug conjugates for cancer therapy. *Nat. Rev. Clin. Oncol.* **18**, 327–344. <https://doi.org/10.1038/s41571-021-00470-8> (2021).
- Verma, S. et al. Trastuzumab emtansine for HER2-positive advanced breast cancer. *N Engl. J. Med.* **367**, 1783–1791. <https://doi.org/10.1056/NEJMoa1209124> (2012).
- von Minckwitz, G. et al. Trastuzumab emtansine for residual invasive HER2-positive breast cancer. *New. Engl. J. Med.* **380**(7), 617–628. <https://doi.org/10.1056/NEJMoa1814017> (2019).
- Li, B. T. et al. HER2-mediated internalization of cytotoxic agents in ERBB2 amplified or mutant lung cancers. *Cancer Discov.* **10**, 674–687. <https://doi.org/10.1158/2159-8290.CD-20-0215> (2020).
- Blair, H. A. Pyrotinib: First global approval. *Drugs* **78**, 1751–1755. <https://doi.org/10.1007/s40265-018-0997-0> (2018).
- Su, B. et al. Apatinib exhibits synergistic effect with pyrotinib and reverses acquired pyrotinib resistance in HER2-positive gastric cancer via stem cell factor/c-kit signaling and its downstream pathways. *Gastric Cancer* **24**, 352–367. <https://doi.org/10.1007/s10120-020-01126-9> (2020).
- Yan, M. et al. Pyrotinib plus capecitabine for human epidermal growth factor receptor 2-positive metastatic breast cancer after trastuzumab and taxanes (PHENIX): A randomized, double-blind, placebo-controlled phase 3 study. *Transl. Breast Cancer Res.* **1**, 13–13. <https://doi.org/10.21037/tbcr-20-25> (2020).
- Collins, D. M. et al. Effects of HER family-targeting tyrosine kinase inhibitors on antibody-dependent cell-mediated cytotoxicity in HER2-expressing breast cancer. *Clin. Cancer Res.* **27**, 807–818. <https://doi.org/10.1158/1078-0432.CCR-20-2007> (2021).
- Köninki, K. et al. Multiple molecular mechanisms underlying trastuzumab and lapatinib resistance in JIMT-1 breast cancer cells. *Cancer Lett.* **294**, 211–219. <https://doi.org/10.1016/j.canlet.2010.02.002> (2010).
- Gymnopoulos, M., Elsliger, M. A. & Vogt, P. K. Rare cancer-specific mutations in PIK3CA show gain of function. *P Natl. Acad. Sci. USA* **104**, 5569–5574. <https://doi.org/10.1073/pnas.0701005104> (2007).
- Zhang, Y., Chen, X., Zhao, Y., Ponnusamy, M. & Liu, Y. The role of ubiquitin proteasomal system and autophagy-lysosome pathway in Alzheimer's disease. *Rev. Neurosci.* **28**, 861–868. <https://doi.org/10.1515/revneuro-2017-0013> (2017).
- Nam, T., Han, J. H., Devkota, S. & Lee, H. W. Emerging paradigm of crosstalk between autophagy and the Ubiquitin-Proteasome system. *Mol. Cells* **40**, 897–905. <https://doi.org/10.14348/molcells.2017.0226> (2017).
- Mayer, M. P. & Bukau, B. Hsp70 chaperones: Cellular functions and molecular mechanism. *Cell. Mol. Life Sci.* **62**, 670–684. <https://doi.org/10.1007/s00018-004-4464-6> (2005).
- Santamaria, S. et al. Imaging of endocytic trafficking and extracellular vesicles released under neratinib treatment in ERBB2 + breast cancer cells. *J. Histochem. Cytochem.* **69**, 461–473. <https://doi.org/10.1369/00221554211026297> (2021).
- Tanner, M. et al. Characterization of a novel cell line established from a patient with Herceptin-resistant breast cancer. *Mol. Cancer Ther.* **3**, 1585–1592. <https://doi.org/10.1158/1535-7163.1585.3.12> (2004).
- Chen, R. H., Chen, Y. H. & Huang, T. Y. Ubiquitin-mediated regulation of autophagy. *J. Biomed. Sci.* **26**, 80. <https://doi.org/10.1186/s12929-019-0569-y> (2019).
- Xu, W. et al. Chaperone-dependent E3 ubiquitin ligase CHIP mediates a degradative pathway for c-ErbB2/Neu. *Proc. Natl. Acad. Sci. USA* **99**, 12847–12852. <https://doi.org/10.1073/pnas.202365899> (2002).
- Citri, A. et al. Drug-induced ubiquitylation and degradation of erbB receptor tyrosine kinases: Implications for cancer therapy. *EMBO J.* **21**, 2407–2417. <https://doi.org/10.1093/emboj/21.10.2407> (2002).
- Birrer, M. J., Moore, K. N., Betella, I. & Bates, R. C. Antibody-drug conjugate-based therapeutics: State of the science. *J. Natl. Cancer Inst.* **111**, 538–549. <https://doi.org/10.1093/jnci/djz035> (2019).
- Barok, M., Tanner, M., Koninki, K. & Isola, J. Trastuzumab-DM1 causes tumour growth inhibition by mitotic catastrophe in trastuzumab-resistant breast cancer cells in vivo. *Breast Cancer Res.* **13**, R46. <https://doi.org/10.1186/bcr2868> (2011).
- Maruyama, T. et al. Lapatinib enhances herceptin-mediated antibody-dependent cellular cytotoxicity by up-regulation of cell surface HER2 expression. *Anticancer Res.* **31**, 2999–3005 (2011).
- Tian, H. et al. Dramatic response to pyrotinib and T-DM1 in HER2-negative metastatic breast cancer with 2 activating HER2 mutations. *Oncologist* **28**, e534–e541. <https://doi.org/10.1093/oncolo/oyad122> (2023).
- Kulukian, A. et al. Abstract P1-18-09: Tucatinib, a HER2-selective tyrosine kinase inhibitor, increases the anti-tumor activity of trastuzumab antibody-drug conjugates in preclinical models of HER2 breast cancer. *Cancer Res.* **80**(4_Suppl), P1–18. <https://doi.org/10.1158/1538-7445.sabcs19-p1-18-09> (2020).
- Boz Er, A. B. & Er, I. Targeting ITGβ3 to overcome trastuzumab resistance through epithelial-mesenchymal transition regulation in HER2-positive breast cancer. *Int. J. Mol. Sci.* **25**. <https://doi.org/10.3390/ijms25168640> (2023).

Author contributions

All authors contributed to the study conception and design. Conceptualization, formal analysis, investigation, methodology, visualization and writing—original draft were performed by W.R.; Conceptualization, funding acquisition, writing—review and editing were performed by T.Z.; Formal Analysis, investigation, methodology and writing—original draft were performed by J.L.; Writing—Review and editing were performed by R.Z.; Investigation were performed by F.Z., Y.Z. and J.M. All authors read and approved the final manuscript.

Funding

This work was supported by the Natural Science Foundation of Hebei Province, China [Grant Number H2013505059].

Declarations

Competing interests

The authors declare no competing interests.

Ethical approval

The animal study protocol was approved by the ethics committee of Bethune International Peace Hospital (protocol code dwsy-22-12-10).

Additional information

Supplementary Information The online version contains supplementary material available at <https://doi.org/10.1038/s41598-025-03678-1>.

Correspondence and requests for materials should be addressed to T.Z. or J.L.

Reprints and permissions information is available at www.nature.com/reprints.

Publisher's note Springer Nature remains neutral with regard to jurisdictional claims in published maps and institutional affiliations.

Open Access This article is licensed under a Creative Commons Attribution-NonCommercial-NoDerivatives 4.0 International License, which permits any non-commercial use, sharing, distribution and reproduction in any medium or format, as long as you give appropriate credit to the original author(s) and the source, provide a link to the Creative Commons licence, and indicate if you modified the licensed material. You do not have permission under this licence to share adapted material derived from this article or parts of it. The images or other third party material in this article are included in the article's Creative Commons licence, unless indicated otherwise in a credit line to the material. If material is not included in the article's Creative Commons licence and your intended use is not permitted by statutory regulation or exceeds the permitted use, you will need to obtain permission directly from the copyright holder. To view a copy of this licence, visit <http://creativecommons.org/licenses/by-nc-nd/4.0/>.

© The Author(s) 2025